

Magnetic MIMO: How To Charge Your Phone in Your Pocket

Jouya Jadianian Dina Katabi
Massachusetts Institute of Technology
{jouya, dk}@mit.edu

ABSTRACT

This paper bridges wireless communication with wireless power transfer. It shows that mobile phones can be charged remotely, while in the user's pocket by applying the concept of MIMO beamforming. However, unlike MIMO beamforming in communication systems which targets the radiated field, we transfer power by beamforming the non-radiated magnetic field and steering it toward the phone. We design MagMIMO, a new system for wireless charging of cell phones and portable devices. MagMIMO consumes as much power as existing solutions, yet it can charge a phone remotely without being removed from the user's pocket. Furthermore, the phone need not face the charging pad, and can charge independently of its orientation. We have built MagMIMO and demonstrated its ability to charge the iPhone and other smart phones, while in the user's pocket.

Categories and Subject Descriptors C.2.2 [Computer Systems Organization]: Computer-Communications Networks

Keywords Wireless Power Transfer, MIMO, Magnetic Resonance, Energy, Beamforming, Mobile and Wearable Devices

1. INTRODUCTION

Wireless power transfer promises to revolutionize mobile computing and enable smart phones and portable devices to be permanently unplugged. Yet, while wireless chargers are now available for many mobile phones, their utility is quite limited. We still need to remember to regularly charge our mobile phones; only instead of inserting the cable every time, we can now put the phone on a charging pad. To many of us, this is not the wireless charging we hoped for. We would like to have our cell phones charged in our pockets, and never again worry about forgetting to charge the phone.

Past work on wireless power transfer, however, cannot deliver this vision. Transferring a significant amount of power wirelessly is typically done via the magnetic field, which is highly directional and its value drops very quickly with distance. As a result, state-of-the-art phone chargers are limited to distances of one or a few centimeters, and require the phone to be perfectly aligned with the charging pad.

Yet, a small increase in the distance and flexibility of wireless charging would translate to a big improvement in the user experience. In particular, many people are office workers who spend multiple hours a day sitting at their desks [9]. It would be highly desirable to have phone chargers that work at distances of about 30 or 40 cm

Permission to make digital or hard copies of all or part of this work for personal or classroom use is granted without fee provided that copies are not made or distributed for profit or commercial advantage and that copies bear this notice and the full citation on the first page. Copyrights for components of this work owned by others than the author(s) must be honored. Abstracting with credit is permitted. To copy otherwise, or republish, to post on servers or to redistribute to lists, requires prior specific permission and/or a fee. Request permissions from permissions@acm.org.

MobiCom'14, September 7-11, Maui, Hawaii, USA.

Copyright is held by the owner/author(s). Publication rights licensed to ACM.
ACM 978-1-4503-2783-1/14/09
<http://dx.doi.org/10.1145/2639108.2639130> ...\$15.00.

and can charge a phone independently of its orientation. One could then attach a charging pad below the desk and use it to charge the user's phone whenever she is sitting at her desk. With such a setup, many of us would hardly ever need to take a phone out of our pocket to charge it. Achieving this vision however is not easy given the directionality and fast drop in the magnetic field.

This paper delivers a system that can charge a cell phone at distances of about 40 cm, and works independently of how the phone is oriented in the user's pocket. Our approach builds on analogous designs common for wireless data communications. Wireless communications use multi-antenna beamforming to concentrate the energy of a signal in a particular direction in space. As a result, these systems can reach longer distances and change the directionality (i.e., orientation) of their signal to focus it on the receiver. Past work on RF beamforming however operates in the far field, where the separation between transmitter and receiver is significantly larger than the wavelength. Wireless charging however operates in the near field, where it relies on the magnetic field for its power transfer. Our aim is to extend the principles of MIMO beamforming to focus the magnetic field in the spatial direction of the phone we want to charge.

Our design, called MagMIMO, enables wireless charging systems to focus their power transfer and beam it towards the phone, in a manner analogous to beamforming in wireless communications. Specifically, state of the art wireless charging uses a technique called inductive resonance [17]. A source coil in the charging pad is used to generate the magnetic field. The phone is equipped with a receiving coil which may be inside the phone's case or in an attached sleeve. When the magnetic field traverses the phone's coil, it generates a current that charges the battery. These two coils are the transmit and receive antennas of the wireless system. Current systems use a single transmit coil and hence the receiving coil in the phone has to be close and well aligned with the transmit coil in the pad to collect the energy in the magnetic field. In contrast, MagMIMO uses multiple coils on the transmitter side in a manner similar to multi-antenna wireless communication systems. The currents in the various coils are coordinated so that their magnetic fields combine constructively at the phone's coil –i.e., create a beam toward the phone. The resulting beam is spatially steered according to the location of the phone.

As in traditional MIMO beamforming, focusing the magnetic field's beam toward the phone requires the source to know the channels.¹ In communication systems this is addressed either by having the receiver measure the channels and send them back to the source, or by listening to some transmission from the receiver and inferring the reciprocal channels [33]. In MagMIMO, we neither need the receiver to directly send us the channels nor to transmit so that we may listen to the reciprocal channels. Because of the magnetic coupling between the transmitter and receiver, our source can measure the parameters for beamforming simply by measuring the load the receiver's circuit imposes on the transmitter's circuit. This enables the

¹Like in RF systems, the channels are complex coefficients that capture how the transmitter's signal is received.

phone to convey the channel information to the power source without extra overhead.

We have built a prototype of MagMIMO and tested it with the iPhone 4s in the aforementioned office set-up. We also compared the prototype against commercial iPhone chargers (i.e., Energizer Qi, Duracell, RAVpower) as well as recent published work (WiTricity 2000M [36], UW prototype [30]). Since these baselines use different input power, we set the combined input power of MagMIMO’s source coils to be about the average input power used by the various baselines. Our results show the following:

- MagMIMO can charge the iPhone at distances up to 40 cm, whereas commercial chargers and academic systems are limited to 1 cm and 10 cm, respectively.
- MagMIMO charging time is lower than all baselines for the same distance. The charging time naturally increases for longer distances. For example at distances of 30 cm, MagMIMO charges the iPhone from a dead battery to a full charge within an average of 4 hours and 50 minutes, which is about twice as much as it takes to charge the iPhone 4s when directly plugged to the power source.²
- MagMIMO can charge the iPhone at any orientations –i.e., from perfect alignment at 0 degree to an orthogonal alignment at 90 degrees. In contrast, all baselines fail at 10 degrees or lower, except WiTricity 2000M [36] which operates up to 30 degrees.
- In experiments run with a population of users who carried their own smart phones while working at a desk, MagMIMO has succeeded in charging the user’s phone independent of whether the user kept the phone in her shirt, pants, or jacket pocket. We have also conducted experiments in which the user placed his or her phone on the desk in a random position, either directly on the surface of the desk, or in a backpack, or on top of other objects (e.g., a book). MagMIMO has succeeded in charging the phone in all of these scenarios. The charging time from a dead battery varied between 2h:53m and 6h:15m, depending on the phone location and the movements of the user.

Contributions: So far, wireless power transfer has been developed in isolation from the vast and powerful literature on wireless communications. By bridging the two research areas, this paper is able to present the first demonstration of wireless charging of a smart phone while in the user’s pocket. This performance is enabled by a novel design that focuses the magnetic flux from multiple coils in a steerable beam and points it at the phone, in a manner analogous to multi-antenna beamforming in wireless communications. The design can charge unmodified smart phones at distances up to 40 cm, and works regardless of the phone orientation with respect to the charging pad.

2. RELATED WORK

Wireless power transfer has been successfully adopted in cell phone chargers [7, 36] and electric car chargers [10]. It is also proposed for charging sensors [12, 19, 11], consumer electronics [25, 20], and medical implants [15, 14, 26]. Practical schemes for charging phones and similar consumer devices however are limited to distances of few centimeters and require the receiver coil to be aligned with the charging pad [7, 8, 27, 36, 25]. Examples of wireless power transfer at longer distances either require a large and heavy receiver coil, as in cars [10], or they can only deliver very little power sufficient to light an LED at \sim 10–200mW [37], but cannot charge a cell phone battery which requires a few Watts [2].

²Note that these numbers are for charging the iPhone starting from a dead battery. For this scenario, it took 2 hours and 15 minutes to charge the phone when directly plugged to the power outlet, which is consistent with previously reported measurements [2].

The literature also has examples of systems that use “multi-coils” but none of these technologies shapes the magnetic flux in a steerable beam, analogous to traditional MIMO beamforming. Past work on multi-coil power transfer falls in three categories: Some schemes use multiple transmit coils but at any time, turn only one coil on – typically the coil closest and most aligned with the receiver coil [10, 23]. Other schemes use passive coils that operate as repeaters [26, 34, 35]. A third category uses one transmitter coil but attempts to power multiple devices each with its own receiver coil [18]. MagMIMO is fundamentally different from these approaches because it actively shapes the combined magnetic flux of the coils as a beam, and dynamically steers this beam towards the receiver to maximize power delivery.

A recent startup named Ossia [39, 31] proposed to power phones remotely using a very large array of WiFi MIMO transmitters. In contrast to all of the above work as well as MagMIMO, which deliver power via the magnetic field, WiFi MIMO delivers power using RF radiation. While RF radiation can be used to deliver a small amount of power as in RFIDs, delivering a large amount of power via radiation can cause local heating inside the human body [22]. This is because radiated power at hundreds of MHz–GHz frequencies can easily be absorbed by water that constitutes majority of the human body [38]. Hence, power transfer technologies have so far avoided operating in the radiation mode. Furthermore, given the limited public information about the technology underlying Ossia, it is unclear how efficient their approach is (meaning how long it takes to charge the phone) and whether the technology obeys the FCC regulations. Nevertheless, the technology is useful for environments in which humans are not present, such as automatic wireless battery charging of sensor networks in an industrial environment. While MagMIMO’s design is inspired by MIMO RF techniques used in wireless communications, MagMIMO is the first technology that provides beamforming of the magnetic field and develops the underlying mathematical formulation and system architecture.

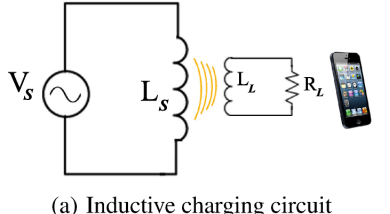
Finally, in §5.3, we use a form of in-band communication to detect the presence of a chargeable phone and adapt to changes in its load. This design is motivated by past work on wireless power transfer that used in-band communication for device discovery (e.g., [16] and [32]), but differs in the details of our communication protocol.

3. PRIMER

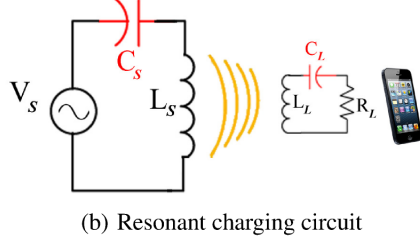
Wireless power transfer systems deliver power via magnetic coupling between the transmitter’s and receiver’s circuits [20]. As shown in Fig. 1(a), a coil of conductive material, e.g., copper, is connected to an AC power source to generate an oscillating magnetic field. A second conducting coil, brought very close to the first, would experience an oscillating magnetic flux. Variations in the magnetic flux traversing the secondary coil induce an electric current, which may be used to power devices like phones.

To increase efficiency, state of the art wireless chargers add a capacitance to both the transmitter and receiver circuits and make them resonate at the same frequency [20, 25], as illustrated in Fig. 1(b). With magnetic resonance, once the source voltage at the transmitter triggers oscillation, the circuit can keep resonating back and forth without consuming extra energy [21]. Of course in practice some of the energy is dissipated in the intrinsic resistance of the coil, but the overall efficiency of power transfer is significantly higher.

It is important to realize that power transfer depends on the amount of magnetic flux traversing the secondary coil, as shown in Fig. 2. In the case of a single transmitter coil, aligning the receiver coil with the source coil maximizes the magnetic flux through the receiver coil and hence the amount of energy delivered to the phone, as in Fig. 2(a). On the other hand, if the receiver coil is orthogonal to the transmitter

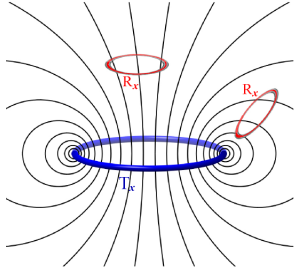


(a) Inductive charging circuit

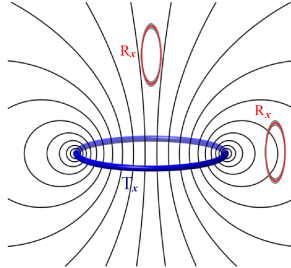


(b) Resonant charging circuit

Figure 1: Illustration of wireless power transfer.



(a) Aligned Tx/Rx coils with maximum flux linkage



(b) Orthogonal Tx/Rx coils with minimum flux linkage

Figure 2: Magnetic flux through the receiver coil and its impact on power transfer. The power transfer is high in (a) where the Tx-Rx coils are aligned and the magnetic flux through the receiver coil is large, but there is zero power transfer in (b) due to perpendicular transmitting and receiving coils.

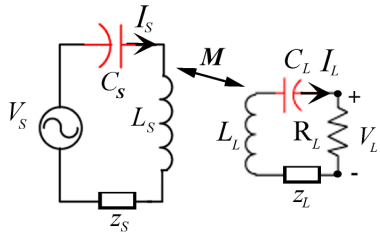


Figure 3: Illustration of a single-Tx-coil power transfer circuit.

coil (on the centerline or on the same plane as the transmitter), no magnetic flux will traverse the receiver coil and hence no energy will be delivered, as in Fig. 2(b).

3.1 Basic Circuit Equations

The above concepts can be mathematically captured via basic circuit equations [38]. Consider the illustration in Fig. 3 which shows the power transmitter and the receiver being magnetically coupled. The term M refers to the mutual inductance between the two circuits, i.e., the amount of magnetic coupling. It depends on the parameters of the two circuits as well as the relative distance and orientation of the coils on both sides. As explained earlier, due to magnetic coupling the transmitter circuit induces a current in the receiver circuit, i.e., it delivers power to the receiver. The resulting receiver current,

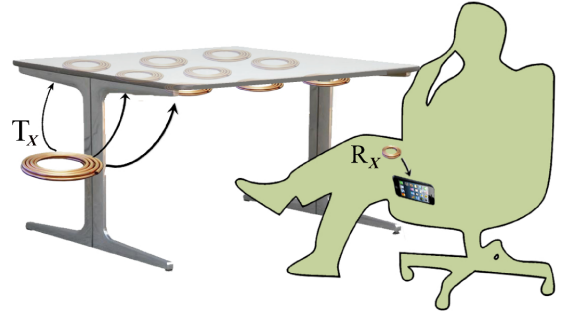


Figure 4: 2-D array of Tx coils, installed underneath an office desk surface, delivers power to Rx coil attached to the phone.

I_L , is a direct function of the magnetic coupling, M , the transmitter current I_s , and the circuit parameters and can be computed using basic circuit equations:

$$I_L(R_L + j\omega L_L + \frac{1}{j\omega C_L} + z_L) = j\omega MI_s, \quad (1)$$

where R_L , L_L , C_L , and z_L are the receiver's resistance, inductance, capacitance, and complex impedance, respectively, and ω is the frequency of the system.

Due to magnetic coupling, not only the transmitter impacts the receiver, but the receiver also impacts the transmitter as follows:

$$V_s = I_s(j\omega L_s + \frac{1}{j\omega C_s} + z_s) - j\omega MI_L, \quad (2)$$

where V_s is the voltage on the transmitter side, I_s is the transmitter current, and L_s , C_s and z_s are the inductance, capacitance and complex impedance of the transmitter circuit.

The above equations are for any frequency ω . However, when the circuit operates at its resonance frequency as they should in a wireless power transfer system, the terms $j\omega L$ and $\frac{1}{j\omega C}$ cancel each other and hence disappear from the above equations.

In the rest of the paper, we use (1) and (2) to derive the magnetic-beamforming relations. As we will see in §5.1, since our design builds a MIMO transmitter, there are multiple transmitter circuits not just one. Hence, the terms MI_s and MI_L in (1) and (2) will be replaced by $\sum M_i I_{si}$ and $\sum M_i I_L$, respectively, where M_i is the mutual inductance between the receiver and the i_{th} source circuit in which current, I_{si} , flows.

4. DESIGN SPECIFICATIONS

MagMIMO is designed to charge phones remotely while a user is setting at her desk, as described in §1. We aim for satisfying distances in the range of ~ 30 cm to 40 cm, and all possible phone orientations, while keeping the input power on par with present wireless chargers.

The transmitter consists of n similar coils deployed underneath the surface of a typical office desk as shown in Fig. 4. The only assumption we have is that the desk surface is not made of conducting metals. The receiving coil is a small coil that can be incorporated either inside the phone or in its sleeve. There are no assumptions on the charged phones. The system works properly with off the shelf smartphones by feeding the charging power through the USB port.

5. MAGMIMO

MagMIMO performs what we call multi-coil magnetic-beamforming, which is analogous to (but not the same as) multi-antenna beamforming in wireless communications. This design concentrates the magnetic flux along a beam, so that the power transfer can reach further distances. It also steers the resulting

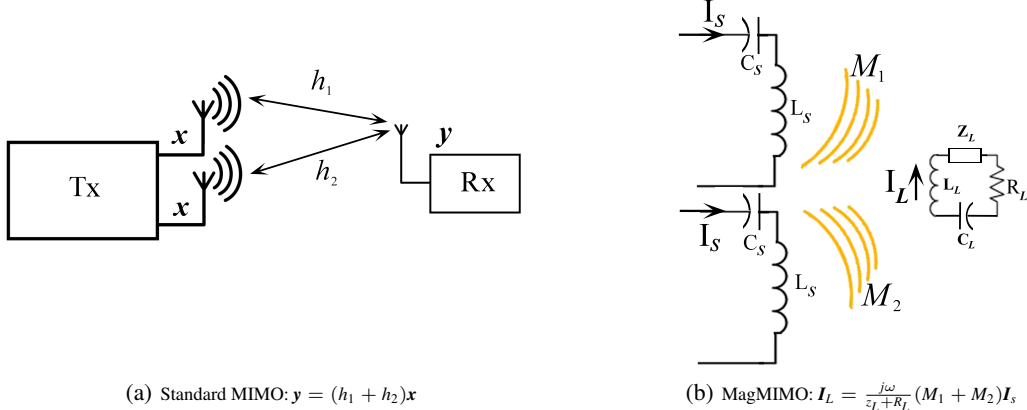


Figure 5: Illustration of the analogies between standard MIMO and MagMIMO: (a) In standard MIMO, the output, y , at the receiver antenna, is a linear combination of the input signal x , where the combiners are the wireless channels, h_1 and h_2 ; (b) similarly in MagMIMO, the current induced in the receiver coil, I_L , is a linear combination of the input current I_s , where the combiners are proportional to the mutual inductances between the receiver and each transmitter, M_1 and M_2 .

beam and adjusts the direction of the magnetic flux to accommodate the orientation of the receiver coil in the phone.

5.1 Magnetic-Beamforming in MagMIMO

In this section, we explain the analogy between the conventional beamforming in communication systems and MagMIMO's magnetic-beamforming. We then leverage that analogy to derive the rules governing magnetic-beamforming.³ For clarity, we consider a 2-antenna MIMO transmitter. Generalization to a larger number of antennas is straightforward.

Consider a standard MIMO transmitter with two antennas as shown in Fig. 5(a). Say we want to beamform the signal x to the receiver. From standard MIMO equations [4], [33], we know that the received signal y can be expressed as:

$$y = (h_1 + h_2)x, \quad (3)$$

where h_1 and h_2 are the wireless channels from the two transmitting antennas to the receiving antenna.

We also know that we can maximize the SNR of y at the receiver by beamforming the transmitted signal x . This is done by using a beamforming vector (α_1, α_2) , and transmitting $\alpha_1 x$ on the first antenna, and $\alpha_2 x$ on the second antenna. By Maximal-Ratio Combining (MRC), the elements of the beamforming vector should satisfy:

$$\alpha_i = \frac{h_i^*}{\sum_{i=1}^n |h_i|^2}, \quad (4)$$

where h_i^* is the complex conjugate of the channel coefficient h_i . Intuitively, the beamforming vectors above ensure that the signal from each antenna is rotated and weighted according to the phase and strength of the channel, such that the signals from all antennas are aligned to maximize the power at the receiver.

Now, consider the power transfer system in Fig. 5(b), where we would like to beam the magnetic field resulting from the two coils on

³Nonetheless, we note that shaping the non-radiated magnetic field as a beam while analogous to traditional beamforming is also quite different from it and cannot be implemented by simply using traditional beamforming. These are two different phenomena: the former operates over the near-field magnetic flux while the latter operates over the far-field propagating waves. Thus, while the analogy is helpful in understanding and developing the design, MagMIMO requires developing a new mathematical formalization that optimizes power transfer.

the transmitter to maximize the power transferred to the receiver's side. Maximizing the power at the receiver means maximizing the current induced in the receiver's coil, I_L . As explained in §3, the transmitter impacts the receiver's current, I_L , via the mutual inductance between the transmitting coils and the receiving coil, as shown in Fig. 5(b). Thus, the mutual inductance plays the role of magnetic channels. Let us refer to the transmitter's current by I_s . Applying basic circuit equations, we can write the current in the receiving coil as a function of the current fed to the transmitting coils. In particular, we can apply (1) while taking into account that we have two transmit coils (instead of just one):

$$I_L(R_L + z_L + j\omega L_L + \frac{1}{j\omega C_L}) = j\omega(M_1 + M_2)I_s, \quad (5)$$

where M_1 and M_2 are the mutual inductances between the receive coil and the two transmit coils; ω is the frequency of AC current at the transmitter; and R_L , z_L , L_L , C_L are the resistance, impedance, inductance, and capacitance on the receiver's side.

The equation above shows that the receiver current, I_L (which is analogous to the received signal y in a MIMO communication system) can be expressed in terms of the source current, I_s (which is analogous to the source symbol x in a communication system). Taking into account that power transfer systems are tuned to the frequency of resonance and hence the terms $\frac{1}{j\omega C_L}$ and $j\omega L_L$ cancel each other out, we can re-write (5) as:

$$I_L = (m_1 + m_2)I_s, \quad (6)$$

where:

$$m_i = \frac{j\omega}{z_L + R_L} M_i. \quad (7)$$

The term m_i is the scaled version of the magnetic inductance between the transmitting coil and receiving coil. We refer to m_i as the magnetic channel between Tx_i and Rx.

Comparing (6) with (3), it is clear that they have the same format. Thus, similar to traditional MIMO beamforming, we can maximize the current induced in the receiver's coil, I_L , by scaling the current flowing in the transmitter's coils I_s with a magnetic-beamforming vector (β_1, β_2) , such that:

$$\beta_i = \frac{m_i^*}{\sum_{i=1}^n |m_i|^2}, \quad (8)$$

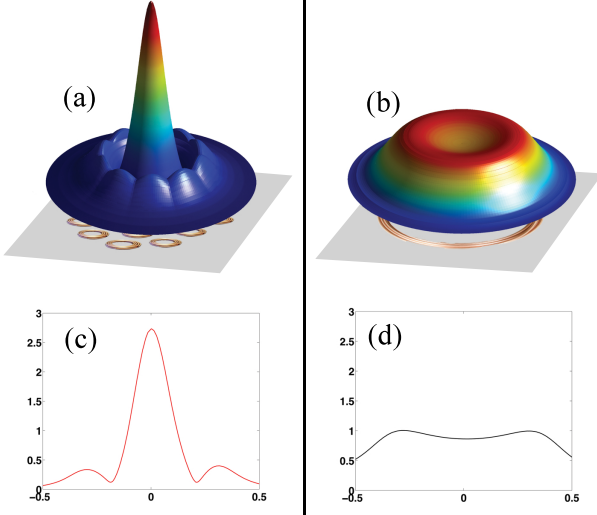


Figure 6: Comparison of the magnetic flux density. The figure plots the magnetic flux in cartesian coordinates resulting from (left): magnetic-beamforming using MagMIMO system and (right): a large single coil. (a) and (b) show the 3-D distribution of the flux density, while (c) and (d) show 2-D planar cuts of quantities shown in (a) and (b), respectively. By comparing left and right panels, it is clear that MagMIMO has effectively focused the field in the desired direction. The occupied area and the input power is the same for both systems.

where m_i^* is the complex conjugate of the magnetic channel m_i , and $\beta_i I_s$ is the current in the transmitter's i^{th} coil.

We note that maximizing the receiver's current, I_L , naturally translates to magnetic-beamforming the field toward the receiver's coil, in a manner similar to how maximizing the received symbol, y , translates to standard MIMO beamforming. This is because the magnetic field amplitude at the receiver coil is proportional to I_L [38]. The proportionality means that maximizing I_L is identical to maximization of the local magnetic flux magnitude at the receiver coil.⁴

To illustrate this relation, Fig. 6 shows the result of MagMIMO's magnetic-beamforming, as expressed in the above equations, and compares it with an omnidirectional magnetic field resulting from a large single coil. The quantity shown in this figure is the magnitudes of the magnetic flux density normalized by the peak of the large single coil's magnetic flux density. The total occupied area and the input power for the single coil and the multiple Tx coils of MagMIMO are the same. The simulation data shown in Fig. 6 are obtained by using AC/DC module of COMSOL Multiphysics [6], a commercial computation packages commonly used for electromagnetic simulations.

As can be seen in this figure, the concentrated magnetic flux generated by MagMIMO magnetic-beamforming is significantly higher than the single coil's magnetic field despite the fact that they consume the same input power. Therefore, MagMIMO has successfully beamformed the magnetic field. The reason that MagMIMO is able to create a higher magnetic flux maximum with the same power as the single coil is that the field is lower at other points in space except on the center line, which is the direction of the receiver in our simulation. Hence, MagMIMO concentrates the input power in the desired direction. The advantage of MagMIMO magnetic-beamforming is even higher than expressed in Fig. 6, since the power delivered to the receiver is proportional to the *square* of the magnetic flux that traverses the receiver coil [38].

⁴In fact y in (3) is the voltage of the receiver antenna that is proportional to the electric field of the incident wave at the receiver, in a similar way that I_L is proportional to the magnetic field at the receiver coil.

Also note that the beam is steered as the receiving coil moves or turns, i.e., changes its location or orientation. This is because the mutual inductances, M_i 's, change with the receiver's location and orientation, similarly to how channels change when the receiver's location changes in MIMO communication systems. In contrast, existing solutions have no way for steering the magnetic flux towards the phone as it changes location or orientation and hence need the phone to be aligned with the charging pad.

5.2 MagMIMO Protocol

This section describes the procedure that MagMIMO follows to beamform its signal to the receiver, and adapt to receiver's movements by steering the beam as needed. The procedure has three steps: channel estimation, magnetic-beamforming, and automatic beam steering, as detailed below.

1. **Magnetic Channel Estimation:** In communication systems, a MIMO transmitter needs to learn the channels from itself to the receiver in order to compute the magnetic-beamforming vector. Similarly, a MagMIMO transmitter needs to learn the magnetic channels to the receiver (i.e., the m_i 's) to compute its magnetic-beamforming vector.

In communication systems, the transmitter obtains the channels either by having the receiver measure the channels and send them back to the transmitter, or by listening to some transmission from the receiver and inferring the reciprocal channels [33]. Unlike communication systems, in MagMIMO, we neither need the receiver to directly send the channels to the source nor to transmit so that the source may listen to the reciprocal channels. Because of magnetic coupling between the transmitter and receiver, our transmitter can estimate the channels simply by measuring the load that the receiver imposes on the transmitter circuit. In particular, from §3.1, the impact of the receiver on each of the transmitter's coils can be captured using (2) as:

$$V_{s_i} = I_{s_i} (j\omega L_{s_i} + \frac{1}{j\omega C_{s_i}} + z_{s_i}) - j\omega M_i I_L, \quad (9)$$

where V_{s_i} and I_{s_i} are the voltage and current of the i^{th} Tx coil. L_{s_i} , C_{s_i} and z_{s_i} are the inductance, capacitance, and impedance of the i^{th} Tx coil, and M_i is its mutual inductance with the receiver's coil.

The above equation can be used to measure the magnetic channels from the transmitter to the receiver. Specifically, periodically, we apply a known voltage, V_{s_i} , to the i^{th} Tx coil, and then measure the current I_{s_i} flowing through the coil while keeping the other transmit coils open circuit. Dividing the known voltage by the measured current gives us the total impedance of the Tx coil, $z'_i = \frac{V_{s_i}}{I_{s_i}}$. Substituting from (9) and given that the system is tuned to the frequency of resonance and hence $\frac{1}{j\omega C_{s_i}}$ and $j\omega L_{s_i}$ cancel out, we have:

$$z'_i = \frac{V_{s_i}}{I_{s_i}} = z_{s_i} - j\omega M_i \frac{I_L}{I_{s_i}}. \quad (10)$$

Since during the channel measurement phase only one Tx coil is active at any time and the other are open circuit, we can use (1) to estimate I_L and substitute it in (10). We can also cancel out $\frac{1}{j\omega C_L}$ and $j\omega L_L$ since the circuit is operating at its resonance frequency, which yield:

$$\omega^2 M_i^2 = (z'_i - z_{s_i})(R_L + z_L), \quad (11)$$

where z'_i is the measured impedance of Tx_i , while other Tx coils are silent, meaning that they are open circuited, and z_{s_i} is the intrinsic impedance of Tx_i .⁵

⁵This impedance represents the total impedance of the transmitter coil in the absence of a receiver, which includes the impedance of

Equation (11) allows the wireless power transmitter to compute the absolute value of the mutual inductance between each of its coils and the receiver's coil, i.e., $|M_i|$. This equation however does not provide the sign of M_i . To determine the sign, one should define a positive direction for a reference coil and compute the sign of the M_i 's with respect to that reference, which we explain in detail in Appendix §A.

Once the absolute value and sign of M_i are known, they are substituted in Equation (7). As a result, the magnetic channel between the i^{th} transmit coil and the receive coil can be computed as:

$$m_i = j\gamma_i \sqrt{\frac{z'_i - z_{s_i}}{R_L + z_L}}, \quad (12)$$

where γ_i is an indicator variable whose value is $+1$ if the sign of M_i is positive and -1 otherwise.

- 2. Magnetic-Beamforming:** Once the magnetic channels are estimated, the optimum beamforming parameters are immediately derived from (8), and the currents of each transmit coil is set to satisfy: $I_{si} = \beta_i I_s$. Assigning these currents to the Tx coils ensures that the beam is accurately steered toward the receiver coil.⁶

Therefore, the way we perform the beam steering in MagMIMO is essentially similar to standard MIMO beam steering. The steering is performed automatically based on the data collected from channel estimation, and then depending on each transmitter's channel, the system selects an appropriate feeding scheme (derived from (8) and (13)) for the optimum wireless charging.

- 3. Automatic Beam Steering:** The phone's position and orientation can change during the charging process, causing the magnetic channels between the transmitter and receiver coils to change. Thus, it is essential that steps 1 and 2 are repeated every few seconds so that MagMIMO is able to re-steer its beam to deliver the optimal power every time the user changes the location and/or orientation of the phone.

5.3 Feedback from the Receiver

Up to this point, we have made two key assumptions: 1) the phone is always present within the reach of MagMIMO and 2) the receiver load resistance is constant. These two assumptions are not necessarily true in practice. The phone may be not in range, in which case, MagMIMO should turn off the charging system to save energy. As for the receiver's load, R_L , it is a function of the battery's instantaneous charge level, and continuously increases as the phone's battery fills up [2], as shown in Fig. 7. Hence, the power transmitter needs to learn the current value of R_L to accurately compute the magnetic channels and the beamforming vector.

the DC voltage supply, amplifier and intrinsic resistance of L_{s_i} and C_{s_i} .

⁶In practice, it is more convenient to apply voltages rather than currents –i.e., use a voltage source. Thus, we can easily compute the source voltages that generate the desired currents, I_{si} , using standard circuit equations as:

$$\begin{pmatrix} V_{s1} \\ V_{s2} \\ \vdots \\ V_{sn} \end{pmatrix} = \begin{pmatrix} z_{s1} & j\omega M_{1,2} & \cdots & j\omega M_{1,n} & j\omega M_1 \\ j\omega M_{2,1} & z_{s2} & \cdots & j\omega M_{2,n} & j\omega M_2 \\ \vdots & \vdots & \ddots & \vdots & \vdots \\ j\omega M_{n,1} & j\omega M_{n,2} & \cdots & z_{sn} & j\omega M_n \end{pmatrix} \begin{pmatrix} I_{s1} \\ I_{s2} \\ \vdots \\ I_{sn} \\ -I_L \end{pmatrix} \quad (13)$$

where V_{si} , z_{si} , I_{si} stand for the voltage, internal impedance, and the current of the i^{th} source circuit, and M_{ij} is the mutual inductance between transmit coils i and j . All of the elements in the right hand side of (13) are either known from the offline tuning of the system or determined after channel estimation and magnetic-beamforming vector calculation. In particular, $I_{si} = \beta_i I_s$ where I_s is the AC current, and $I_L = \sum m_i I_{si}$.

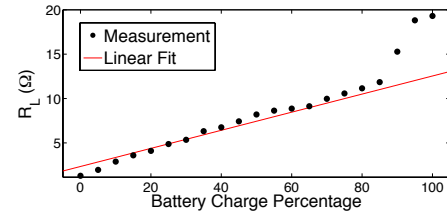


Figure 7: Changes in R_L as the phone charges.

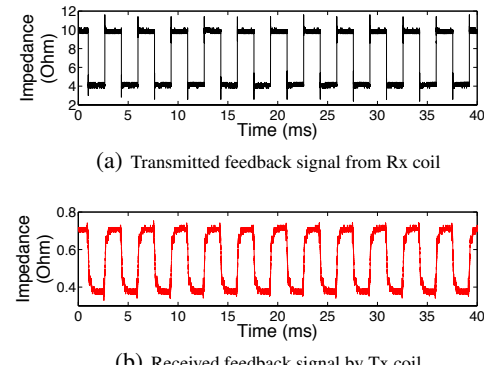


Figure 8: Feedback sent from Rx and received by Tx. The width of the pulse encodes the value of R_L and the presence of the pulse train conveys that a phone equipped with a MagMIMO receiver is in reach of the MagMIMO's transmitter.

In this section, we explain how MagMIMO employs feedback communication from the receiver to detect the presence of the phone and the current value of the load resistance. One option for sending this feedback is to use out-of-band communication via some low power radio, e.g., Bluetooth. This solution is undesirable since it needs an additional radio on the charger and may not work if the phone is completely discharged. In MagMIMO, we send the feedback in-band by having the receiver modulate the power transfer signal, in a manner similar to how RFIDs communicate with their reader.

We leverage the coupling between the transmitter and receiver, due to which changes in the impedance of the receiver's circuit translate to proportional changes in the reflected impedance at the transmitter. Thus, in MagMIMO, the receiver measures R_L and communicates its value to the transmitter by turning a switch on and off to change the reflected impedance. The value of R_L is encoded in the width of the pulse. The pulse is repeated multiple times for reliability. Fig. 8 shows the pulses transmitted from the power receiver and how they are received at the power transmitter. The example in the figure is for R_L equal to 8.25Ω .

On the other side, Tx coil uses the presence of the pulse train as an indication that a phone is within the reach and it needs power. It also finds out the value of R_L by decoding and measuring the pulse width. Note that the Tx can immediately discover the impact of switching the impedance at the receiver due to the coupling between Tx and Rx.

The R_L estimation and in-band communication is repeated every few minutes (every 5 minutes in our prototype). Whenever the value of R_L changes, the channels are updated according to (12).

The above feedback approach is very energy efficient and does not add too much complexity to the system. All of the measurements and modulations on the Rx side are done using the energy harnessed from the transmitter, not the phone's battery. Therefore, MagMIMO works seamlessly even for a completely discharged phone.



Figure 9: MagMIMO prototype. The figure shows the transmit coils placed on a regular office desk; the receiver coil is attached to the back of the phone.

6. PROTOTYPE IMPLEMENTATION

We built a prototype of MagMIMO using off-the-shelf components (Fig. 9). The transmitter can be attached to a regular office desk with metallic, plastic and wood contents. The only restriction of the system is that the desk surface must not be conductive. The receiver circuit has a small coil and can be attached to the back of the phone. It charges unmodified phones via the USB port.

The prototype resonates at a single frequency of 1.0 MHz. The electromagnetic compatibility constraints have been followed so that the MagMIMO prototype is compliant with FCC regulations (both part 15 and part 18). Note, however, that while the prototype operates at this particular frequency, magnetic-beamforming for power transfer is independent of the frequency.⁷

Our implementation, illustrated in Fig. 10, has three components:

1. The transmitter can be powered from a standard 60 Hz power outlet. The transmitter circuit consists of six⁸ transmitting coils (Tx_i) resonating with their own serial capacitors. The area of each Tx coil is 0.05 m^2 which is powered by its own tunable power amplifier (A_i). The transmitting coils and power amplifiers are specifically designed and built to have low resistive and switching losses, respectively. The transmitter occupies the total area of 0.38 m^2 on a regular office desk and is fed by 20 W combined input power across all coils.

The MagMIMO transmitter adjusts both amplitude and phase of the current in each Tx coil in accordance with the description in §5.2. Adjustments of both phase and magnitude are necessary since the magnetic-beamforming vectors are complex numbers (see Equation 8). The amplitude is updated by controlling the voltage at the input of the amplifier and the phase is updated using controllable phase shifters. The details of the circuit are as follows: The phase and amplitude of each coil's voltage are calculated based on equations 8-13 by a microcontroller. The microcontroller then updates the amplitude

⁷Generally, frequencies in the range of hundreds of kHz to a few tens of MHz are suitable for wireless charging [5]. For example, Qi, Duracell, and RAVpower operate at a few hundred kHz [7, 27, 8], Witricity operates at 6.78MHz [36], and the UW prototype sweeps the frequencies from 8 to 22 MHz [30, 29].

⁸Magnetic-beamforming can be used with a different number of coils similarly to how traditional beamforming can operate with a different number of antennas. The larger the number of coils the narrower the beam and the better the performance. As we show in the result section, a choice of 6 Tx coils increases the charging range to 40 cm and can support any phone orientation. We also ran experiments with only two coils. Such a system has an approximately 15% higher charging range compared to a single Tx coil and cannot support all phone orientations.

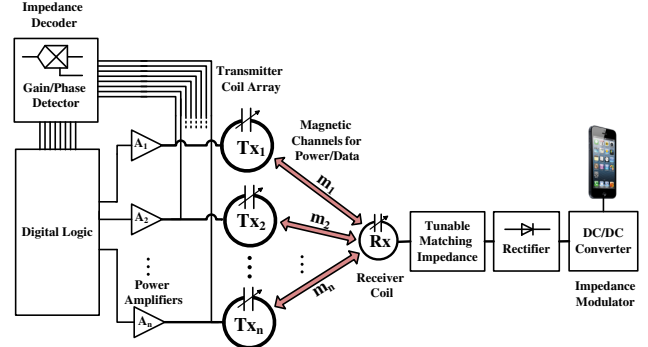


Figure 10: Block diagram of MagMIMO prototype. The magnetic channels, m_1, m_2, \dots, m_n , are estimated by measuring the reflected Rx impedance at each Tx coil. The digital logic controls the currents in the Tx coil array. The matching impedance circuit, rectifier and DC/DC converter condition the voltage and current of the load/receiver.

by changing the magnitude of the DC input of a controllable DC-DC buck converter, and updates the phase using controllable phase-shifter. The resulting voltage controls a DC-AC inverter similar to that in [28] and applies the desired voltage to the respective Tx coil. The combination of these three blocks, “DC-DC converter, Phase shifter, DC-AC inverter,” is the block referred to as “amplifier” in Fig. 10 (i.e., A_1, A_2, \dots, A_6).

2. The receiver coil is quite small with an area of 0.005m^2 and a thickness of a few millimeters. Hence, it can be easily incorporated into the sleeve of the phone. The receiver’s circuit consists of a self-tuning matching circuit, full bridge rectifier and a DC/DC converter attached to the Rx coil resonating with a high Q capacitor. The Rx circuit is connected to the phone’s USB port and hence can be incorporated with unmodified phones.
3. The digital logic component periodically estimates the channels between the transmit coils and the receiver by measuring the impedance of each Tx coil with the aid of a gain/phase detector (Fig. 10). In addition, the logic control system is always listening for the feedback signal transmitted from the receiver. After each channel estimation and feedback reception, the logic component controls the currents that feed the Tx coils to beamform the magnetic field and steer it toward the phone. Once the phone is out of reach, i.e., all the channels are weaker than the threshold and the feedback signal is no longer received, the control logic disconnects the input power, and enters the sleep mode. Only feedback detection remains active in this mode to detect a new receiver.

We have used off-the-shelf components to build the prototype. An ordinary AC/DC converter has been used to convert the 60-Hz electricity from the outlet to feed the Class-E single GaN switch power amplifiers [28] which in turn feed the transmitting coils. To build the resonating Tx and Rx coils, we have used general-purpose copper tubings with diameters of $1/8''$ and $1/16''$, respectively. We have used ultra low Equivalent Series Resistance (ESR) microwave ceramic capacitors. The detailed specifications of the used components are in the Appendix §B. The entire prototype costs less than \$100.

7. EVALUATION

We empirically evaluate MagMIMO and compare its performance with and the performance of state-of-the-art wireless chargers.

7.1 Baselines

We compare the MagMIMO with the following systems:

Table 1: Input power for different wireless charging solutions

Technology	Input Power (W)
RAVpower	7.5
Duracell Powermat	18
Energizer Qi	22
WiTricity WiT-2000M	24
UW Prototype	30
Large Single Coil	20
Selective Coil-Array	20
MagMIMO	20

- Three of the best commercially available wireless chargers: Duracell Powermat [7], Energizer Qi [8], and RAVpower [27].
- Two of the state-of-the-art magnetic resonance prototypes, i.e., WiT-2000M [36] and UW prototype [30]. These two prototypes are not publicly available. Therefore the data for these two cases have been extracted from [36] and [30], respectively.
- A large single transmit coil with a total area equal to the total area of MagMIMO’s six Tx coils.
- A selective coil-array, which uses the same six Tx coils used by MagMIMO. However instead of employing the MagMIMO protocol to set the Tx currents in the coils, this system assigns the total input power to the best coil out of the six Tx coils –i.e., the coil that delivers the highest power to the receiver. To identify the best coil for each measured receiver position, we try each coil in a round robin manner, and report the result for the coil that delivers the maximum power at the receiver.

Table 1 lists the input power consumed by each of the compared systems. Since, the compared baselines differ in their input power, we set MagMIMO’s total input power to the median of the compared system. Note that MagMIMO input power is lower than Energizer Qi, WiT-2000M, and the UW prototype.

7.2 Testing Environment

The system is shown in Fig. 9. The MagMIMO’s coils are placed on the desk only for illustration purposes. In operational mode, Tx coils are placed underneath the surface. We have used a regular iPhone 4s as the testbench cellphone. We have not made any software or hardware modifications on the phone. We simply used its USB port to charge it. The phone and the receiver circuit, attached to its back, have been held with an adjustable plastic arm which easily provides different distances and orientations, as shown in Fig. 9. All tests are run in a standard office environment, while people are working at their desks and naturally moving around.

7.3 Charging as a Function of Distance

We evaluate the ability of MagMIMO to deliver power as the distance between the transmitter and the receiver increases, and compare the performance with the aforementioned baselines. We measure the distance between the receiver and the transmitter as the length of the shortest straight line that connects the Rx coil to the nearest Tx coil. Note that this is a conservative measure of distance (i.e., we underestimate the distance) because it is measured between the nearest parts of the transmitter and receiver as opposed to the centers of the transmitter and the receiver (which are more separated due to the area of coils). In each run, we measure the time it takes the charging system to fully charge the iPhone 4s starting from a dead battery. We repeat the same experiments for MagMIMO, the large single Tx coil, the selective coil array and the commercial chargers. In each run, we move the receiver to a different location in the 3D

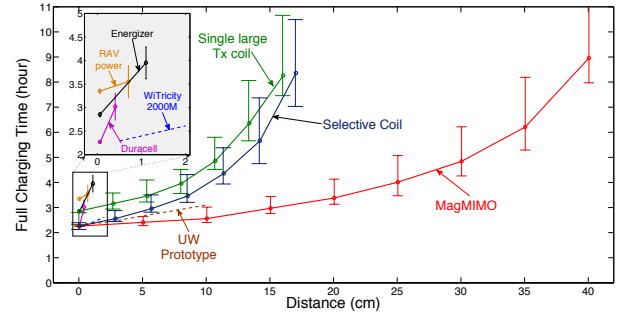


Figure 11: Charging from a dead battery as a function of distance. For each case, the phone has been placed at different distances from the pad to test the time that it takes for the phone to fully charge. All three commercially available wireless chargers simply do not provide any distance beyond 1 cm.

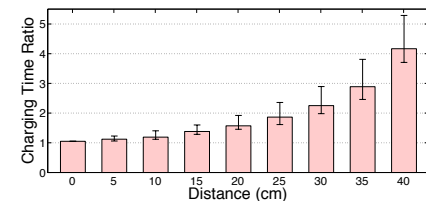


Figure 12: Charging time ratio. MagMIMO wireless charging time divided by wired (plugged-in) charging time.

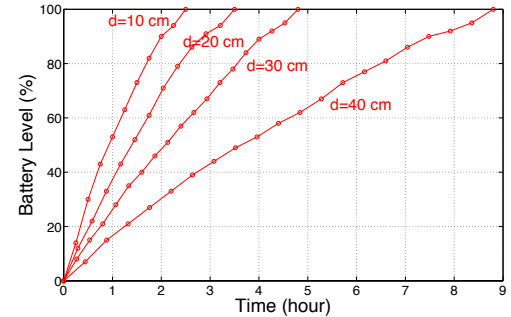


Figure 13: Change in battery level as MagMIMO charges the phone.

space around the transmitter, using the flexible phone holder shown in Fig. 9. We also compare with WiT-2000M [36] and the UW prototype described in [30]. However, since these prototypes are not publicly available, our comparison with these systems is based on the results reported by their designers in [36] and [30], respectively.

Fig. 11 plots, for each system, the charging time starting from a dead battery as a function of the distance between the transmitter and receiver. The error bars show the minimum and 90th percentile of the charging time. The figure reveals the following: First, MagMIMO charging time is smaller than the baselines at any distance for which the baselines are functional. Second, MagMIMO significantly increases the maximum charging distance. MagMIMO maximum charging distance is 40 cm. In comparison, the commercial chargers and WiT 2000M fail to charge the phone at distances of one to two centimeters, whereas the UW prototype, and the single coil, fail at 10 cm and 15 cm respectively. The selective coil-array, which similarly to MagMIMO uses six coils, fails at a distance of 17 cm. This range is significantly lower than that of MagMIMO, which demonstrates the benefits of MagMIMO’s magnetic-beamforming over a best coil design. Third, as expected, in all systems, the charging time increases with distance. For example, when the separation between

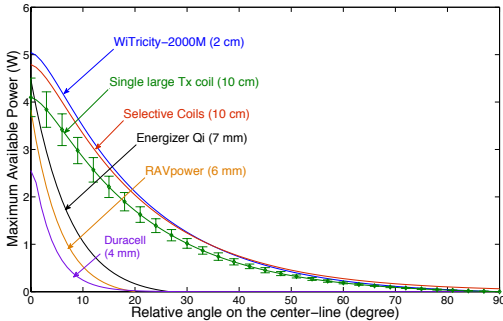


Figure 14: Output power as a function of orientation angle. For the large single Tx coil (at 10 cm) and WiT-2000M (at 2 cm), the maximum available output power from Rx coil significantly drops beyond 30°. The situation is even worse for three of the best commercial wireless chargers (Duracell at 4 mm, RAVpower at 6 mm and Energizer at 7 mm all on the centerlines), as the available power is negligible for angles larger than ~10°.

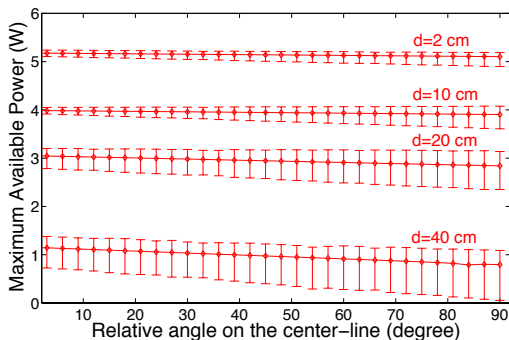


Figure 15: Output power as a function of orientation angle. MagMIMO using collaborative magnetic-beamforming between Tx coils is able to deliver maximum power to the Rx circuit in all situations even if Rx is orthogonal to one of the Tx coils.

the transmitter and receiver is 30 cm, it takes MagMIMO 4 hours and 50 minutes to charge the phone from a dead battery to full charge.

One may also wonder how MagMIMO’s charging time compares with charging the phone by plugging it to the power outlet. In our experiments, plugged-in charging takes 2 hours and 15 minutes to charge the iPhone 4s from a dead battery to a full charge. This number is consistent with prior measurements in the literature [2]. Based on these measurements, we plot in Fig. 12 the ratio of MagMIMO’s charging time to plugged-in charging, for different distances. The figure shows that up to 10 cm, the time taken by MagMIMO is on par with plugged-in charging. At 25 cm to 30 cm, MagMIMO takes twice as much time to charge the phone in comparison to plugged-in charging. The ratio becomes 3 to 4 times for longer distances.

The above numbers provide an upper bound on the charging time. Most users rarely charge the phone from a completely dead battery. In particular, Fig. 13 shows the charge in the battery as a function of the charging time. This figure enables the reader to estimate how much time it takes to charge the phone between two specific battery levels, for a particular distance. For example, to charge the iPhone’s battery from 30% to 80% full, MagMIMO takes about 1.5 hours at 20 cm and 2.5 hours at 30 cm.

7.4 Charging as a Function of Orientation

Next, we evaluate the ability of MagMIMO to charge the phone independent of its orientation with respect to the charging pad, and compare it with the various baselines. We measure the orientation

Table 2: Charging the phone in the user’s pocket

Number of users	Range (cm)	Avg. time (h:mm)	Comments
3	10–30	4:30	Working on a laptop
3	15–25	3:50	Reading a book
1	20–40	5:50	Phone in shirt’s pocket
2	20–30	5:10	Phone in jacket’s pocket
2	20–40	6:15	Moving very often

Table 3: Charging the phone on the desk

Number of users	Avg. time (h:mm)	Comments (Average number of movements)
6	2:53	Phone placed on the desk surface (3)
2	3:40	Phone contained in a purse/bag (9)
3	3:27	Phone placed on another object (7)

of the receiver with respect to the transmitter as the minimum angle between the planes created by the transmitter coil(s) and the receiver coil. We empirically measure the performance as a function of orientation for MagMIMO, the selective coil-array, the large single Tx coil, and the commercial chargers. We also compare with WiT-2000M based on their specification sheet. However, we cannot compare with the UW prototype since [29, 30] do not provide information about how they address orientation for phone charging.⁹

We note that since the compared schemes do not support the same distance, we could not fix one distance and compare all schemes. Thus, for the baselines we plot the performance as a function of orientation, for their operational distances. For MagMIMO, we plot in the performance as a function of orientation, for a variety of distances up to 40 cm.

Figs. 14 and 15 compare the performance dependency of different systems on the relative angle between the receiver coil (Rx) and the transmitter coil(s) (Tx pad). The horizontal axis of this figure shows the relative angle and the vertical axis shows the power delivered to the receiver at that specific relative angle.

The results in Fig. 14 show that, for the baselines, the maximum available power strongly depends on the relative angle between the phone and the charging pad. For the large single Tx coil (at 10 cm), like other single coil technologies, the available power significantly drops beyond 30°. The same is true for the WiT-2000M (at 2 cm), which uses a similar technology. The selective coil-array (at 10 cm) is not any better despite its use of multiple coils. The situation is much worse for three of the best commercial wireless chargers, as the power is negligible for angles larger than ~10°.

In contrast, Fig. 15 shows that MagMIMO is able to deliver a consistent power level to the phone in all situations even if it is orthogonal to the Tx coils. This is due to MagMIMO beam-steering capability which allows it to adapt the direction of the magnetic flux according to the orientation of the phone. Compare MagMIMO’s performance with the selective coil-array, which although adapts the choice of coil according to the receiver’s position, it does not have a beam-steering capability and as a result it cannot charge the phone as its orientation gets more orthogonal to the charging pad.

7.5 User Experiments

We have performed experiments with a population of users to validate that MagMIMO can indeed charge a user’s phone while she is working at her desk. We also validate that MagMIMO works with different smartphone models.

In each experiment, a different user was asked to attach the receiver circuit to his/her own smartphone and keep it in his/her pocket,

⁹The paper shows orientation results only for large receive coils which cannot be attached to a phone.

Table 4: MagMIMO’s transfer efficiency at different distances

Distance	0.5 cm	2 cm	5 cm	10 cm	20 cm	30 cm	40 cm
Efficiency	89%	87%	74%	53%	34%	19%	11%

while sitting normally at the desk. The user can keep other objects in the same pocket with the phone, e.g., coins, keys, etc. The phone screen was checked for its battery level every few minutes. The smartphones used herein are Samsung Galaxy SIII, 2×Apple iPhone 4s, 2×Apple iPhone 5s, Samsung Galaxy S III, 2×Samsung Galaxy S4, Samsung Galaxy Note II, Motorola Droid Ultra, and LG Lucid 2. The phones were charged from a dead battery to a full charge.

The results in Table 2 show that MagMIMO always succeeded in charging the user’s phone independent of the phone’s type and whether the user kept the phone in her shirt, pants, or jacket pocket.

Some users like to keep their phones on the desk to check messages and notifications. Thus, we conducted experiments in which we asked the users to put their phones wherever they want on the desk. The users were allowed to keep the phone in their back-pack or purse, or to put the phone on top of any nonmetallic object instead of directly putting it on the desk surface. The users were also allowed to change the position of their phone any time as they wish. Table 3 shows that MagMIMO succeeded in charging the phone in all of these scenarios with an average charging time between 2h:53m and 3h:40m.

7.6 Power Transfer Efficiency

The transfer “efficiency” is the received power at the Rx coil divided by the total input power at the Tx coils. We measured the efficiency of MagMIMO for varying distances in the range [0.5 cm, 40 cm]. Table 4 reports MagMIMO’s average efficiency as a function of the distance, where the average is taken over different phone orientations. The efficiency of MagMIMO at a close distance is 89%. The efficiency at tens of centimeters may look low, however to the best of our knowledge, our efficiency numbers are the highest for magnetic resonance at such distances with a small receiver coil that fits in the back of a phone. In particular, the Witricity baseline is reported to have a maximum efficiency of 86% for distances less than 2cm [36], which is lower than MagMIMO. [36] does not report the efficiency at distances larger than 2cm. However, since it cannot charge a phone beyond 2cm (while MagMIMO can), one can conclude that the efficiency at such distances is smaller than MagMIMO.

Note that the size of the Rx coil is a determining factor for efficiency, since one can always collect more magnetic flux using a larger Rx coil. Past papers that reports higher efficiency at distance use large Rx coils unsuitable for a phone. For example, [17] achieves higher efficiency but uses a 3-D Rx coil whose diameter is 60 cm and has a depth of 20 cm, making it unsuitable for our application.

7.7 Impact of Charging on Temperature

We have measured the temperature rise on MagMIMO’s Tx and Rx coils as well as the commercially available wireless chargers using a temperature gun infrared thermometer [24]. Over a period of seven hours, the maximum temperature rise for MagMIMO is 2°C when the system performs at its maximum power. For the commercially available wireless chargers, however, the temperatures rises to an uncomfortable level. Over seven hours the temperature rises of 23°C, 22°C, and 16°C were measured for Energizer, RAV power and Duracell, respectively. Therefore, MagMIMO’s operation over

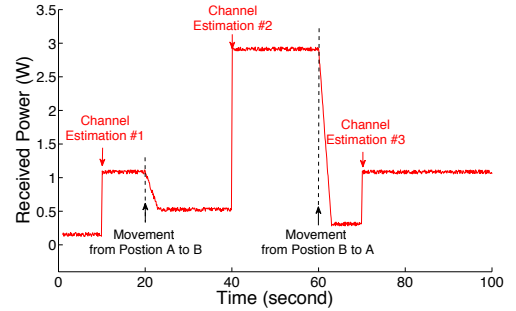


Figure 16: Microbenchmark for channel estimation and magnetic-beamforming performance. A receiver has been moved from position A at $t=20$ s to position B, and then again back to position A at $t=60$ s. MagMIMO performs channel estimation and magnetic-beamforming every 30 seconds starting from $t=10$ s. The figure shows the role of channel estimation and beam steering in adapting to movements.

long periods of time results in a temperature rise that is $10\times$ smaller than the baselines over the same period of time.¹⁰

7.8 Microbenchmark

Next, we focus on the performance of the individual components of MagMIMO and how they contribute toward its effectiveness.

Channel Estimation. To investigate the effectiveness of MagMIMO’s channel estimation, we perform a series of experiments, in which the receiver (load) moves during the experiment from one position to another causing a change in the magnetic channels. Fig. 16 illustrates one of these experiments in which the phone is moved from position A (at 38 cm from Tx) to position B (at 22 cm from Tx), and then again from position B back to position A. The figure plots the power delivered to the phone over time. As can be seen in this figure, MagMIMO adapts to changes in the channels; the received power is significantly raised due to magnetic-beamforming at every channel estimation at $t=10$ s, 40s and 70s.

Feedback. To validate the effectiveness of feedback communication in MagMIMO we perform a set of experiments with and without feedback. Figure 17 plots the results of a representative example, where MagMIMO has been powering a load (placed at 30 cm from Tx) that abruptly changes on 5 occasions (C1–C5). In particular, R_L starts from 5Ω , and each time it is increased by 2Ω . The instantaneous received powers of the system with and without feedback communication are plotted against time on top/red and bottom/black profiles, respectively. For both sets of the results in Fig. 17, the channel estimation is enabled and all other parameters of systems are exactly similar.

As can be seen in Fig. 17, the feedback from the receiver helps MagMIMO better estimate the load and hence have more accurate channel estimates. In the absence of such feedback the performance can severely drop due to inaccurate load value, which leads to inaccurate channel estimates.¹¹

8. CONCLUDING REMARKS

¹⁰We also note that it is safe to touch the MagMIMO coils even if they are not insulated. We have measured the touching voltage showing that the touch voltage is always under 10 volts, which is way lower than the safety threshold [13].

¹¹The reason why the power slightly degrades even in the presence of the feedback is that the impedance matching hardware is optimal only within a certain range. This is a hardware limitation independent of the accuracy of the feedback.

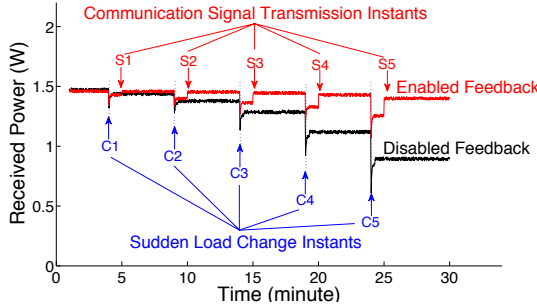


Figure 17: Microbenchmark of feedback communication. The load is made to abruptly change at C1–C5. The figure shows that the feedback transmitted by the receiver at S1–S5 is properly used to update the next beamforming matrix, resulting in a raise in received power level to deal with the change in the load. In contrast, the system with disabled feedback suffers a significant loss whenever the load deviates from the presumed value.

This paper introduces MagMIMO, a system that charges portable devices such as cell phones at distances up to 40 cm and independently of the device’s position and orientation, while commercial chargers and academic systems are limited to less than 10 cm. MagMIMO achieves this by adapting the wireless communication concept of MIMO beamforming to concentrate the resonating magnetic field on the receiver device to maximize the power transfer efficiency. Evaluation of MagMIMO’s prototype proves that it makes a significant improvement both in the reliability and efficiency of the wireless power transfer. Finally, we note that MagMIMO does not require any modification to the phone and hence can be used with today’s phones by incorporating the small receiver coil (and circuit) in a sleeve attached to the phone. In future work, we envision extending MagMIMO to support simultaneous charging of multiple devices, in a manner analogous to the multi-user MIMO technique. We will also consider extensive user studies that explore the typical distance between a working user and her desk, and the impact of MagMIMO’s improved range and flexible orientation on the user experience.

Acknowledgments: We thank Omid Abari, Fadel Adib, Arthur Berger, Diego Cifuentes, Ezz Hamed, Haitham Hassanieh, Zack Kabelac, Swarun Kumar, Hariharan Rahul, Lixin Shi, Deepak Vasisht, Jue Wang and our reviewers for their insightful comments. This research is funded by NSF. We thank members of the MIT Center for Wireless Networks and Mobile Computing: Amazon, Cisco, Google, Intel, Mediatek, Microsoft, ST Microelectronics, and Telefonica for their support.

9. REFERENCES

- [1] Analog Devices Inc. datasheet for AD8302 LF-2.7 GHz gain and phase detector.
- [2] Apple Inc. *Rechargeable Li-based Batteries*, 2013.
- [3] Arduino. Uno datasheet. <http://arduino.cc/>.
- [4] D. W. Bliss, K. W. Forsythe, and A. M. Chan. MIMO Wireless Communication. *Lincoln Lab, MIT*, 2005.
- [5] F. Carobolante. Wireless power transfer, overcoming the technological hurdles. In *APEC*. IEEE, 2014.
- [6] COMSOL Inc. *Reference guide 4.3b*, 2013.
- [7] Duracell Corp. *PowerMat Technologies*, 2011.
- [8] Energizer. Qi-Enabled 3 Position Inductive Charger.
- [9] Ergotron Inc. *To Sit or Stand? Almost 70% of Full Time American Workers Hate Sitting, but They do it all Day Every Day*, 2013.
- [10] S. Hasanzadeh, S. Vaez-Zadeh, and A. H. Isfahani. Optimization of a Contactless Power Transfer System for Electric Vehicles. *IEEE Trans. Vehic. Tech.*, 2012.
- [11] L. He, Y. Gu, J. Pan, and T. Zhu. On-demand charging in wireless sensor networks: Theories and applications. In *WASA*, 2010.
- [12] L. He, Y. Gu, J. Pan, and T. Zhu. On-demand charging in wireless sensor networks: Theories and applications. In *IEEE Conf. on Mobile Ad-Hoc and Sensor Systems*, 2013.
- [13] IEC. Standard 60364: Electrical installations for buildings. Part 1: Low-voltage electrical installations.
- [14] S. Kelly, P. Doyle, A. Priplata, O. Mendoza, and J. L. Wyatt. Optimal primary coil size for wireless power telemetry to medical implants. In *ISABEL*, 2010.
- [15] S. Kim, J. S. Ho, and A. S. Y. Poon. Wireless power transfer to miniature implants: Transmitter optimization. *IEEE Trans. Antennas Propag.*, 2012.
- [16] S.-H. Kim, Y.-S. Lim, and S.-J. Lee. Magnetic resonant coupling based wireless power transfer system with in-band communication. *Journal of Semiconductor Technology and Science*, 13(6):562–568, 2013.
- [17] A. Kurs, A. Karalis, R. Moffatt, J. D. Joannopoulos, P. Fisher, and M. Soljacic. Wireless power transfer via strongly coupled magnetic resonances. *Science*, 2007.
- [18] A. Kurs, R. Moffatt, and M. Soljacic. Simultaneous mid-range power transfer to multiple devices. *Applied Physics Letters*, 96(4):044102, 2010.
- [19] K. Li, H. Luan, and C.-C. Shen. Qi-ferry: Energy-constrained wireless charging in wireless sensor networks. In *IEEE Wireless Comm. and Networking Conf.*, 2012.
- [20] M. Kesler, Witricity Corp. *Highly Resonant Wireless Power Transfer*, 2013.
- [21] H. Mohseni, J. Jadidian, A. A. Shayegani-Akmal, E. Hashemi, A. Naieny, and E. Agheb. In-situ insulation test of 400 kV GIS. *IEEE Transactions on Dielectrics and Electrical Insulation*, 15(5):1449–1455, 2008.
- [22] J. Nadakuduti and P. G. L. Lu. Operating frequency selection for loosely coupled wireless power transfer with respect to RF emissions and exposure. *IEEE Wireless Power Transfer Conf.*, 2013.
- [23] F. S. A. Note. Low-power wireless charger transmitter design using MC56F8006 DSC.
- [24] Omega Inc. Temperature gun infrared thermometers.
- [25] Qualcomm. WiPower Technology.
- [26] A. K. RamRakhiani and G. Lazzi. Multicoil telemetry system for compensation of coil misalignment effects in implantable systems. *IEEE Antennas and Wireless Propagation Letters*, 11:1675–1678, 2012.
- [27] RAV Power. datasheet for Qi-Enabled Charger.
- [28] L. Roslaniec and D. J. Perreault. Design of variable-resistance class E inverters for load modulation. *IEEE ECCE*, 2012.
- [29] A. P. Sample, D. Meyer, and J. Smith. Analysis, experimental results, range adaptation of magnetically coupled resonators for wireless power transfer. *IEEE Trans. Ind. Electron.*, 2011.
- [30] A. P. Sample, B. H. Waters, S. T. Wisdom, and J. R. Smith. Enabling Seamless Wireless Power Delivery in Dynamic Environments. *IEEE Proceedings*, 2013.
- [31] TechCrunch. Cota by ossia aims to drive a wireless power revolution and change how we think about charging, 2013.
- [32] Texas Instruments. Qi compliant wireless power transmitter manager.
- [33] D. Tse and P. Vishwanath. *Fundamentals of Wireless Communications*. Cambridge University Press, 2005.
- [34] B. Wang, W. Yerazunis, and K. H. Teo. Wireless power transfer: Metamaterials and array of coupled resonators. *Proceedings of the IEEE*, 101:1359–1368, June 2013.

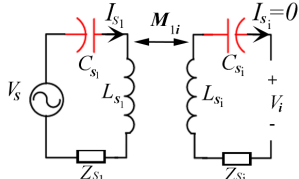


Figure 18: Off-line calibration between Tx coils

- [35] H. Wang. Multiple-resonator magnetic resonant coupling wireless power transfer. Master's thesis, University of Pittsburgh, Pittsburgh, PA, Feb. 2012.
- [36] Witricity Corp. *Developers Kit for Mobile, data sheet “WiT-2000M”*, 2013.
- [37] Witricity Corp. *Prodigy: a hands-on demonstration system*, 2014.
- [38] M. Zahn. *Electromagnetic Field Theory: A Problem Solving Approach*. Hillsdale, N.J. : L. Erlbaum Associates, 1990.
- [39] H. Zeine. *Patent Application: Wireless Power Transmission System*. US 2012/0193999 A1, 2012.

APPENDIX

A. COMPUTING THE SIGN OF M_i

The signs of the M_i 's are defined with respect to some reference Tx coil. Let us pick the first Tx coil as the reference. In this case, M_1 is positive by definition, and we are interested in computing the sign of M_i for the other Tx coils. (Note that we could have defined M_1 to be negative, in which case all M_i 's would flip sign, and hence the voltages induced by the Tx coils at the receiver coil will all flip sign, without any change in the power delivered to the receiver).

The computation of the sign of M_i involve two steps:

(a) One-time Calibration Step: The objective of this step is to compute the mutual inductance between Tx_1 (the reference coil) and Tx_i , i.e., M_{1i} . Since this value is independent of the receiver and does not change over time, it can be computed by the manufacturer offline, in the absence of any Rx coil.

To compute M_{1i} , we apply a source voltage V_s on the first Tx coil (the reference), and leave all other Tx coils open-circuit, as shown in Fig. 18. The figure focuses only on the part of the circuit that involves Tx_1 and Tx_i , and ignores the other Tx coils (which is feasible because they are open circuit). Since the circuit operates at its resonance frequency, the terms involving L and C cancel each other. Further, $I_i = 0$ since the Tx_i coil is left open circuit. Using the basic circuit equations (i.e., KVL), we write:

$$V_s = I_{s1}Z_{s1} \quad (\text{applying KVL to } Tx_1) \quad (14)$$

$$V_i = j\omega M_{1i}I_{s1} \quad (\text{applying KVL to } Tx_i) \quad (15)$$

The above two equations yield:

$$M_{1i} = \frac{V_i}{V_s} \cdot \frac{Z_{s1}}{j\omega}, \quad (16)$$

where V_s and Z_{s1} are known, ω is the resonance frequency, and V_i is directly measured. Hence, the above equation provides the value of M_{1i} .

(b) Online Step to Compute the Sign of M_i : As stated in §5.2, Equation (11) provides us with the absolute value of M_i for any i , but not its sign. We also know the sign of M_1 is positive. Hence we know M_1 fully. We also know M_{1i} from the initial calibration step. Given this information, we can measure the sign of M_i as follows: In the presence of the receiver, and during the channel estimation procedure, we apply the source voltage on Tx_1 (the reference coil), while leaving all other Tx coils open circuit, as shown in Fig. 19. Applying

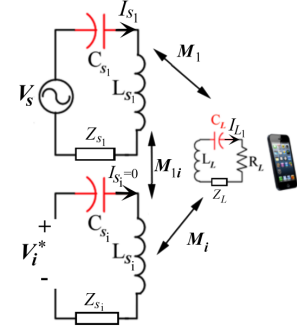


Figure 19: Determining the sign of Tx-Rx mutual inductance

basic circuit equations (i.e., KVL) to the receiver coil yields:

$$j\omega M_1 I_{s1} = I_{L1}(R_L + Z_L) \quad (17)$$

By rearranging the above equation we obtain:

$$I_{L1} = \frac{j\omega M_1 I_{s1}}{R_L + Z_L} \quad (18)$$

Next, we apply KVL to the Tx_i coil, which yields:

$$V_i^* = j\omega M_{1i} I_{s1} + j\omega M_i I_{L1}. \quad (19)$$

We can substitute I_{L1} from (18) in the last equation to obtain:

$$j\omega M_i = \frac{V_i^* - j\omega M_{1i} I_{s1}}{I_{L1}}. \quad (20)$$

In the above equation, all values are known, except for the sign of M_i . Specifically, V_i^* and I_{s1} can be directly measured at the transmitter. M_{1i} is known from the calibration step, and I_{L1} can estimated from (18), where all other values are known. Hence we can determine the sign of M_i as:

$$\text{Sign}(M_i) = \text{Sign}\left(\frac{V_i^* - j\omega M_{1i} I_{s1}}{j\omega I_{L1}}\right). \quad (21)$$

We note two points. First, since mutual inductances are real numbers (no imaginary part), the sign above is well-defined, i.e., the value on the right hand side of the equation inside the sign function is real and has a well-defined sign. Second, the reader may wonder why we do not use Equation (20) to directly determine the magnitude of M_i as well as its sign. The reason is that I_{L1} is typically small and hence sensitive to measurement errors. Since we divide by I_{L1} , the measurement error can be large and hence the exact value of M_i based on the above equation is less accurate than the value based on (11).

B. OFF-THE-SHELF COMPONENTS USED IN THE MAGMIMO PROTOTYPE

We have designed six tunable single switch power amplifiers based on the description of [28]. The power amplifiers are synchronized every 30 seconds by the digital logic through switch drivers [28], when the system estimates each individual channel by shutting down other Tx coils. The digital logic uses an Arduino micro-controller [3]. Six gain/phase detector ICs (AD8302: 2.7 GHz RF/IF [1]) report the voltages, currents and impedances of all coils to the digital logic at any given time. The pulse train on the receiver side is generated by a SiT1534 ultra low power oscillator. Resonance capacitors are ultra low ESR AVX corporation ceramic capacitors (3.6KV 5% NP0 3838), which provide high Q at high voltages, with negligible loss and temperature rise. To build the Tx and Rx coils, we have used generic refrigeration copper tubings.